



“Gheorghe Asachi” Technical University of Iasi, Romania



---

## EQUILIBRIUM AND KINETIC STUDIES OF METHYL ORANGE ADSORPTION ONTO CHEMICALLY TREATED OIL PALM TRUNK POWDER

Akil Ahmad<sup>1,2</sup>, Mohd Rafatullah<sup>1\*</sup>, Mohammadtaghi Vakili<sup>3</sup>, Siti Hamidah Mohd-Setapar<sup>2</sup>

<sup>1</sup>Division of Environmental Technology, School of Industrial Technology, Universiti Sains Malaysia, Penang 11800, Malaysia

<sup>2</sup>Centre of Lipids Engineering and Applied Research (CLEAR), Universiti Teknologi Malaysia,  
81310 UTM Skudai, Johor, Malaysia

<sup>3</sup>Green Intelligence Environmental School, Yangtze Normal University, Chongqing, 408100, China

---

### Abstract

In the present work, acid treated natural oil palm trunk powder (OPTP) has been utilized as novel adsorbents for the removal of methyl orange (MO) from aqueous solution. The batch method was employed to study the adsorption behavior of MO which was subsequently determined by UV/Visible spectrophotometer. The adsorption characteristics and operational parameters were determined by monitoring different parameters such as pH, contact time, dye concentration and temperature. The acid treated OPTP and MO saturated OPTP adsorbent were characterized based on Fourier transform infrared spectroscopy (FT-IR) and scanning electron microscopy (SEM). The maximum adsorption of MO was observed at pH 6 and a contact time 120 min was sufficient to attain the equilibrium. The adsorption of MO onto treated OPTP best fit to Langmuir model and followed the pseudo second order kinetic model. Different thermodynamic parameters such as free energy, enthalpy, and entropy have been calculated and it was concluded that with increase in temperature adsorption increases, which indicates adsorption of MO onto OPTP was endothermic in nature and favourable with positive value of  $\Delta H^\circ$ . The method can be applied to the removal of MO dyes in waste waters.

*Key words:* adsorption isotherm, equilibrium, kinetic parameter, methyl orange dye, oil palm trunk powder

*Received:* November, 2014; *Revised final:* April, 2015; *Accepted:* April, 2015; *Published in final edited form:* December 2018

---

### 1. Introduction

In recent years, huge amounts of dyes and pigments are directly discharged into the hydrosphere which has adverse effect in environment as dyes give water undesirable colour, reduce sunlight penetration and are objectionable for drinking and other uses (Gupta et al., 2012a; Machado et al., 2012). The source of these discharge are mainly textile, food, paper, plastics, rubber, cosmetic, pharmaceutical industries etc. Most of the dyes are toxic in nature and have carcinogenic, teratogenic and mutagenic effects. Therefore, these coloured effluents need to be treated

properly before the discharged into the water bodies. Among all the dyes, methyl orange (MO) is well known acidic dye (azo dye) which is soluble in water and widely used in the textile, printing, paper manufacturing, pharmaceutical, food industries and also frequently used in research laboratories as the pH indicator (Ayar et al., 2007).

Many physical and chemical methods have been employed for wastewater treatment including coagulation, flocculation, precipitation, adsorption, membrane filtration, photo-catalytic degradation and electrochemical techniques (Demarchi et al., 2016, Litic et al. 2017; Malik and Sanyal, 2004; Mittal et al.,

---

\* Author to whom all correspondence should be addressed: e-mail: mohd\_rafatullah@yahoo.co.in; mrafatullah@usm.my; Phone: +604-653 2111; Fax: +604-653 6375

2009a, 2009b, 2010a; Saleh and Gupta, 2012). Among all the methods, adsorption process appears to be best and efficient method for the removal of environmental pollutants, which are more effective and economical as well (Allen et al., 2004). Various low-cost agricultural waste biomass has been used for the adsorption process, namely spruce wood shavings (Janos et al., 2016), de-oiled soya (Mittal et al., 2005), rice straw (Gong et al., 2008), activated carbon (Tan et al., 2007), pinus bark powder (Ahmad, 2009), tomato plant root and green carbon (Kannan et al., 2009), meranti sawdust (Ahmad et al., 2009), blue green algae (Abou-El-Souod and El-Sheekh, 2016), bottom ash and de-oiled soya (Mittal et al., 2010b), skin almond waste (Atmani et al., 2009), seashell waste (Suteu and Rusu, 2012), sawdust and sawdust-fly ash (Lucaci and Duta, 2011), aspergillus niger dead biomass (Cretescu et al. 2010) etc. But new, economical, easily available and highly effective dye adsorbents are still needed to investigate for the scavenging of dye from water and wastewater.

Out of several agricultural wastes, different parts of oil palm biomass such as trunks, leaves, empty fruit bunches and shell have been widely used as adsorbents for the removal of different kind of pollutants. It has gained attention due to locally available, economical and potential and effective adsorbents for the removal of various inorganic and organic pollutants. The oil palms (*Elaeis guineensis*) are cultivated mainly in South East Asia (Malaysia, Indonesia, and Thailand), Africa (Nigeria and Cameroon), America, and several southern provinces of China. Nowadays, 4.49 million hectares of land in Malaysia is under oil palm cultivation, producing 17.73 million tons of palm oil and 2.13 tons of palm kernel oil (Ahmad et al., 2011). Malaysia is one of the largest producers and exporters of palm oil in the world, accounting for 11% of the world's oils and fats production and 27% of export trade of oils and fats. This fruit peel of cactus is considered as solid waste and has no economic value and use of CFP as an alternative low cost adsorbent will help to reduce the cost of solid waste disposal and environmental contamination.

The aim of this study was to determine the potentiality and adsorption capacity of chemically treated OPTP as adsorbent for the removal of MO dye from aqueous solution by systematic evaluation using a set of parameters such as pH, contact time, concentration, temperature effect and the mechanism of dye adsorption was discussed. The adsorption kinetics (pseudo-first-order, pseudo-second-order and intraparticle diffusion) and isotherm studies (Langmuir, Freundlich and Temkin) for MO adsorption onto OPTP are also studied.

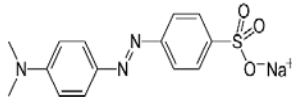
## 2. Materials and methods

### 2.1. Materials

All the chemicals used were of analytical grade reagents and were obtained from Sigma-Aldrich and

Fluka (Germany). A stock solution of methyl orange (MO) (1000 mg/L) was prepared and used as adsorbate and solutions of various concentrations were obtained by diluting the stock solution with distilled water. The pH was adjusted using 0.1 M NaOH and 0.1 HCl solutions. The characteristics of the dye are listed in Table 1.

**Table 1.** Various physical and chemical properties of adsorbate (MO) and adsorbent (OPTP)

Properties	Values
BET surface area (m <sup>2</sup> /g)	1.391
Langmuir surface area (m <sup>2</sup> /g)	2.129
Single point surface area at P/P <sub>0</sub> (m <sup>2</sup> /g)	1.154
Average pore diameter (Å)	72.42
BJH adsorption average pore diameter (Å)	148.25
Single point total pore volume (cc/g)	0.0025
BJH cumulative adsorption pore volume (cc/g)	0.0028
Chemical structure	
Chemical formula	C <sub>14</sub> H <sub>14</sub> N <sub>3</sub> O <sub>3</sub> SNa
Wave length (nm)	464
IUPAC name	Sodium 4-[(4-dimethylamino)phenyl]diazene-2-sulfonate
Molecular weight (g/mol)	327.33
Solubility	Soluble in hot water

### 2.2. Preparation of adsorbent

The natural oil palm trunk was collected from Kedah, Malaysia. Prior to use, the oil palm trunk was washed with double distilled water to remove the adhering dirt. The adsorbent material was kept in an oven for 48 h at 80° C to dry it completely. After that, material was grinded and sieved to desirable particle size ranges from 150–200 µm. 20 g powdered material was treated with 250 mL of 1 M H<sub>2</sub>SO<sub>4</sub>. It was then filtered and washed with double distilled water. The material was further washed with 1 M HNO<sub>3</sub> and then again rinsed with double distilled water to remove the acid. It was further dried in an oven for 24 h at 80° C and used as such for adsorption studies. Finally, chemically activated natural oil palm trunk powdered was kept for adsorption studies.

### 2.3. Characterization of adsorbent

BET surface area of OPTP was measured at 303 K using a static volumetric system ASAP 2020 surface area and pore size analyser (Micrometrics Inc., USA). FTIR spectra of acid treated and MO saturated OPTP adsorbents were recorded using a FTIR Spectrometer (Perkin Elmer 1730, USA) in the region

of 500-4000 cm<sup>-1</sup> at a resolution of ± 4.0 cm<sup>-1</sup>. SEM images were recorded to find the change in the surface morphology of OPTP before and after saturated with MO by Carl-Zeiss SMT (Oberkochen, Germany) scanning electron microscope.

#### 2.4. Batch adsorption studies

Batch experiments for adsorption of MO dye were carried out in conical flask. For this experiment, 0.2 g adsorbent was taken into 100 mL capacity of conical flask with varied concentration of MO solution (50 to 250 mg L<sup>-1</sup>) and final volume of solution was maintained up to 50 mL. The respective dye solution with adsorbent was shaken in water bath shaker at 200 rpm. The effect of pH on the adsorption of MO dye onto OPTP biosorbents was examined in the pH range of 1–8. The pH of the test solutions was maintained by using 0.1M HCl and 0.1M NaOH solution. Moreover the biosorption experiments were also carried out by varying time interval (5.0–240 min) at 200 mg L<sup>-1</sup> concentration to optimize the equilibrium time for the removal of MO from aqueous solution. UV-vis spectrophotometer was used to determine the final concentration of MO dyes in the supernatants solution after the biosorption onto the adsorbents. The biosorption capacity for MO onto OPTP was calculated with the help of following equation (Eq. 1):

$$q_e = \frac{(C_o - C_e) \times V}{M} \quad (1)$$

where,  $C_o$  and  $C_e$  are the initial and equilibrium concentration of MO in the solution, respectively.  $V$  is volume in (L) and  $M$  is the mass of biosorbent (g).

### 3. Results and discussions

#### 3.1. Characterization

BET surface area, Langmuir surface area and total pore volume were determined from the N<sub>2</sub> adsorption data while pore size distribution was calculated based on differential pore volume of BJH adsorption-desorption. The relevant data are presented in Table 1. BET surface area and BJH cumulative adsorption pore volume were found to be 1.391 m<sup>2</sup>/g and 0.0028 cc/g respectively. From the results, OPTP pores are suitable for the removal and separation of MO dye from the aqueous solutions. Scanning electron microscope was used to study the surface morphology of OPTP before and after adsorption of MO, which are shown in Fig. 1.

As shown in Fig. 1a, the surfaces of OPTP are cave like, porous and amorphous structure. However, after adsorption of MO, the surface morphology of MO-loaded OPTP (Fig. 1b) has been changed which is entirely different from the OPTP surface due to adherence of MO dyes on to the OPTP adsorbents, authenticating the adsorption of MO dyes on to the surface of adsorbent.

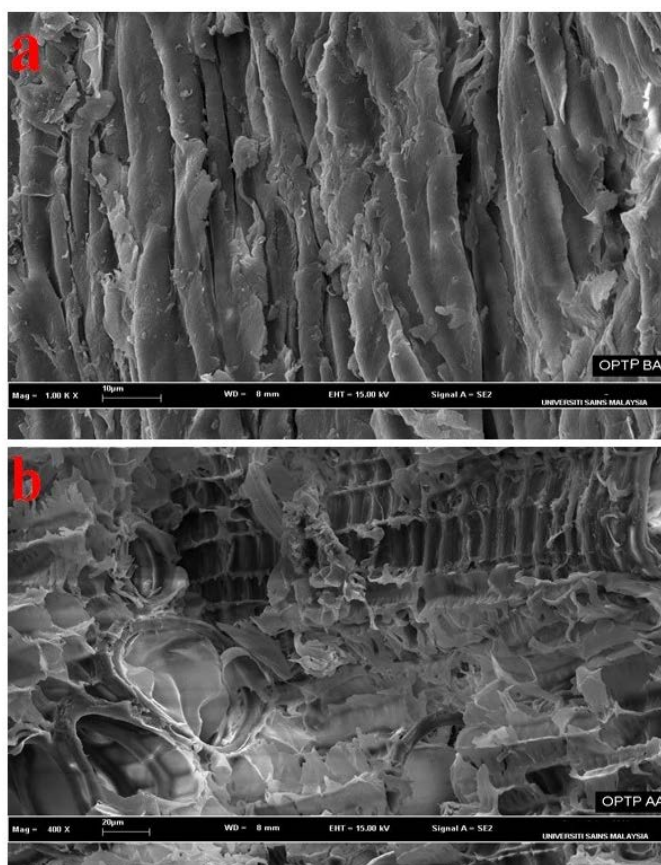


Fig. 1. SEM micrograph of OPTP (magnification: 1000); (a) before adsorption (b) after adsorption

The FTIR analysis was performed for the qualitative determination of the main functional groups present on the surface of OPTP before and after adsorption of MO dyes. The FTIR spectrum of the OPTP is shown in Fig. 2. As shown in Fig 2a, a broad and strong peak appears around  $3421\text{ cm}^{-1}$  was mainly attributing to hydroxyl (O–H) group of the cellulosic part of the OPTP materials. The peak appeared at  $2927\text{ cm}^{-1}$  was assigned to the aliphatic CH groups. Furthermore, the sharp peak appeared at  $1732$  and  $1606\text{ cm}^{-1}$  due to the carbonyl group (C=O) of ester and C=C aromatic ring stretching vibrations (Sjöström, 1981). Whereas the peak at  $1507$  in the spectrum of OPTP may be due to C=C of aromatic rings. The peak at  $1457\text{ cm}^{-1}$  corresponds to the  $\text{CH}_2$  bending vibration. The peaks in the region from  $1317$ – $1231\text{ cm}^{-1}$  may be attributed to the O–H bending and C–OH bending vibrations. The absorption band at  $1158\text{ cm}^{-1}$  corresponds to C–O antisymmetric bridge stretching of cellulosic moiety of OPTP powder. In

Fig. 2b, a strong new peak appeared at  $1046\text{ cm}^{-1}$  due to sulfonic group belongs to MO dye which confirms that MO dyes adsorb on the surface of OPTP adsorbents. As shown in Fig 2b, functional groups of MO loaded OPTP are slightly affected in their position and intensity.

Table 2 lists the shift in wavenumbers observed for COOH and OH stretching frequencies, indicating their role as active sites in binding with the functional groups of the MO (Kumar and Barakat, 2013; Mondal et al., 2014).

### 3.2. Effect of pH and adsorption mechanism

The influence of pH on the adsorption of MO dyes on acid treated OPTP was investigated in the pH range of 1–8 as shown in Fig. 3. Adsorption process is highly dependent on the solution pH, may be due to change of surface charge of adsorbents and ionization of dye molecules.

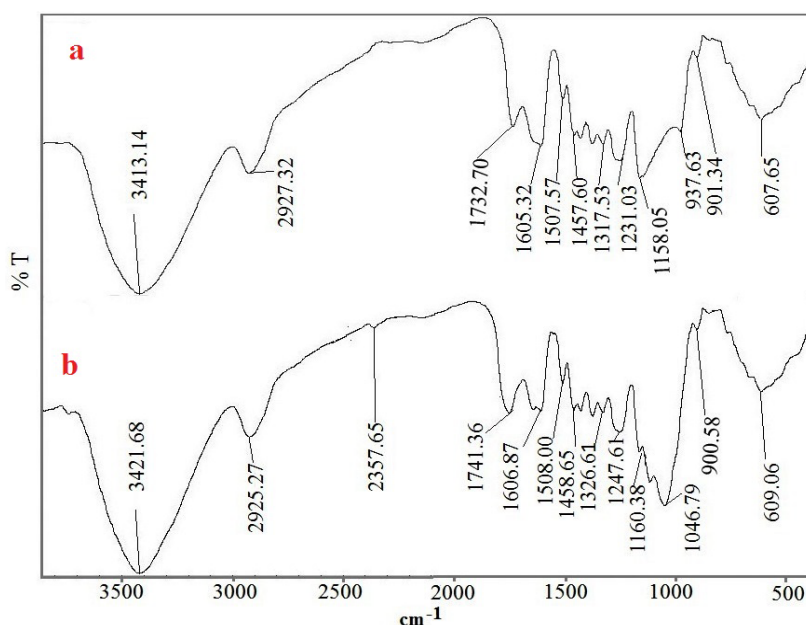


Fig. 2. FTIR Spectra of OPTP; (a) before adsorption (b) after adsorption

Table 2. FTIR spectra of untreated and treated OPTP with MO dye

S. No.	Frequency ( $\text{cm}^{-1}$ )		Differences	Peak Assignment
	Before adsorption	After adsorption		
1	3413	3421	8	O-H (stretching) of phenol group of cellulosic part, lignin and hemicellulose
2	2927	2925	-2	C-H (stretching) of aliphatic compounds, methyl group
3	1732	1741	9	C=O (stretching) carbonyl group of ester
4	1605	1606	1	C=C aromatic ring stretching vibrations
5	1507	1508	1	C=C (aromatic rings)
6	1457	1458	1	$\text{CH}_2$ (bending vibration)
7	1317	1326	9	O-H (bending)
8	1231	1247	16	C-OH (stretch)
9	1158	1160	2	C-O (antisymmetric bridge stretching) of cellulosic moiety
10	-	1046	-	Sulfonic group
11	901	900	-1	C-O-C, C-H deformation and stretching

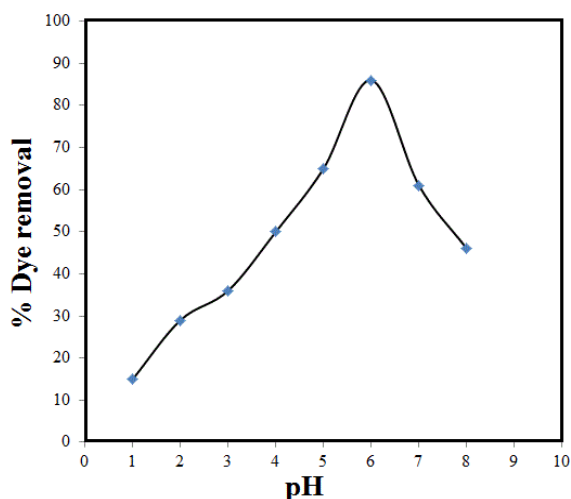


Fig. 3. Effect of solution pH on MO adsorption

Adsorption of MO dye onto OPTP increased with the increase in solution pH and maximum adsorption capacity was examined at pH 6, but decreases when pH is increased further. The maximum adsorption capacity was observed in acidic medium may be due to more positive charge on the adsorbent surface. Same type of works was also revealed by the authors (Ahmad and Kumar, 2010). The adsorption of MO onto OPTP can be elucidated via Vander Waals, electro static, H-bonding and hydrophobic-hydrophobic interactions. In acidic medium, owing to protonation of hydroxyl (-OH) and carboxylic (-COOH) group occurs which present at the surface of OPTP adsorbents likely to be interacted with negatively charged  $\text{SO}_3^-$  of MO dyes. It may be due to the electrostatic interaction between positively charged adsorbents surface and negatively charged

sulfonic group of MO dyes. Other possibility of interaction is H-bonding which occurs between nitrogen and oxygen containing functional group of OPTP surface and MO dyes. Several researchers have also studied the effect of pH on adsorption of MO by using various adsorbent. The optimum pH for MO adsorption was found in the range of 5-6 (Cheah et al., 2013; Hosseini et al., 2011).

Many factors that may influence the adsorption behavior such as dye structure and size, adsorbents surface properties. The sorption of MO onto OPTP can be take place through various kind of faces such as of H-bonding and steric effect, electrostatic and vander Waals interactions etc. MO is a cationic dye having quaternary ammonium and sulphonic groups and the resonance structure of MO is shown in Fig. 4a. The FTIR analysis of OPTP showed that carboxyl and hydroxyl groups are present in abundance on the surface. The carboxylic and hydroxyl groups of adsorbent form the hydrogen bond with the nitrogen containing functional groups of the MO. And under acidic condition, the surface of OPTP get protonated which may bind electrostatically through the negatively charge dye ( $-\text{SO}_3^-$ ) as shown in Fig 4b. Wang and Wang (2008) also reported that the  $-\text{N}=\text{N}$ ,  $-\text{HN}-\text{N}$  and  $-\text{SO}_3$  groups of MO were involved in the adsorption.

### 3.3. Effect of contact time and initial dye concentration

The effect of contact time for the adsorption of MO onto OPTP adsorbents is shown in Fig. 5. The experiment were carried out ranging from 5-240 min, under the same condition of 30 °C, pH 6.0 and the initial concentrations of MO was from 50–250 mg/L.

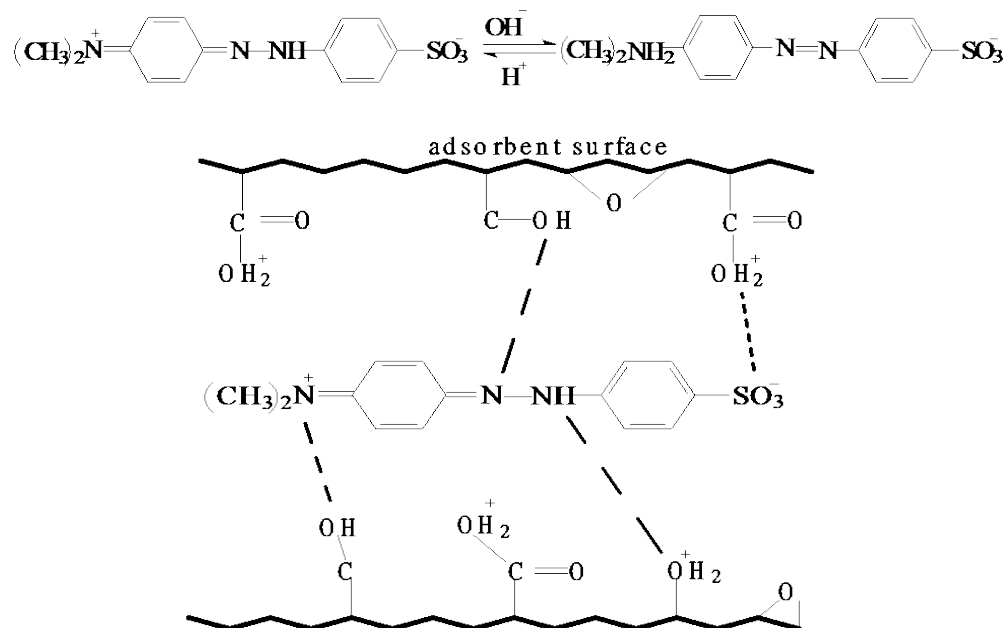


Fig. 4. (a) Resonance structure of MO (b) MO adsorption mechanism onto OPTP (at pH 6)

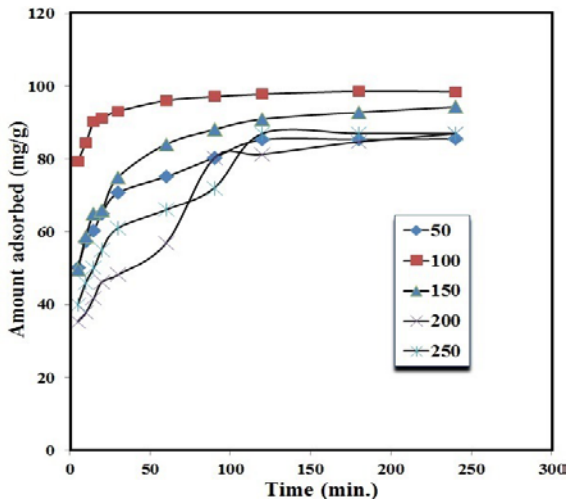


Fig. 5. Effect of contact time and initial concentration on MO adsorption

Initially the uptake rate of MO by OPTP adsorbents increases with the increase in the contact time and the solution concentration. This may be associated to greater driving force of the concentration gradient with the increase in the initial MO concentration (Ashtoukhy, 2009; Hameed et al., 2008). As shown in the time curve, uptake of adsorbate is fast but it gradually slows down until it reaches the equilibrium. This is due to the fact that a large number of vacant surface sites are available for adsorption during the initial stage, and after a lapse of time the remaining vacant surface sites are difficult to be occupied due to repulsive forces between the solute molecules on the solid and bulk phases. The maximum removal of MO onto OPTP adsorbent was obtained after 120 min contact time and remained constant after equilibrium. Once the equilibrium attained, the sorption of MO was constant with further increases of time. Therefore, it was assumed that longer treatment might not have further effect to change the properties of the adsorbent. With the increase of initial dye concentration from 50 to 250 mg/L, the adsorption capacity of OPTP increased from 35.0 to 98.0 mg/g. From the Fig. 5, it was observed that at high

concentrations the fractional adsorption of MO onto OPTP is low, while at low concentrations the initial uptake of dye is rapid, indicating a rapid surface reaction. Therefore, the concentration will greatly affect the extent and rate of MO uptake on OPTP adsorbent. A similar phenomenon was observed for the adsorption of MO onto De-oiled Soya (Mittal et al., 2007) and Coal powder (Zhuannian et al., 2009).

### 3.4. Kinetic studies

In order to determine the adsorption rate of MO dye onto the OPTP surface, pseudo-first order (Lagergren, 1898), pseudo second order kinetic (Gupta et al., 2011b; McKay and Ho, 1999) and Weber-Morris diffusion models (Weber and Morris, 1963) were examined. The linear equation for pseudo-first order kinetic models can be expressed as Eq. (2):

$$\log(q_e - q_t) = \log q_e - \frac{k_1 t}{2.303} \tag{2}$$

where,  $q_e$  is the amount of solute adsorbed at equilibrium per unit weight of adsorbent ( $\text{mg g}^{-1}$ ) and  $q_t$  is the amount of solute adsorbed at any time ( $\text{mg g}^{-1}$ ) and  $k_1$  ( $\text{min}^{-1}$ ) is rate constant. The values of the kinetics parameters were calculated from linear plots  $\log(q_e - q_t)$  Vs  $t$  (Fig. 6a) and summarized in Table 3. From the result, value of  $R^2$  is very low, so it did not follow the Pseudo-first-order kinetic model.

Therefore, the kinetic data was further investigated by using the pseudo-second order model. The linearized form of equation is expressed as Eq. (3):

$$\frac{t}{q_t} = \frac{1}{k_2 q_e^2} + \frac{t}{q_e} \tag{3}$$

where  $q_t$  is the amount of MO dye adsorbed ( $\text{mg g}^{-1}$ ) at given time  $t$  (min),  $q_e$  is the amount of MO dye adsorbed at equilibrium ( $\text{mg g}^{-1}$ ) and  $k_2$  is pseudo-first and pseudo-second order rate constant for adsorption ( $\text{g mg}^{-1} \text{min}^{-1}$ ).

Table 3. Pseudo-first-order, pseudo-second-order and intraparticle diffusion models for the adsorption of MO onto OPTP

Kinetic Models and its Parameters	Initial Concentrations (mg/L)				
	50	100	150	200	250
<b>Pseudo-first-order kinetic</b>					
$q_e$ (mg/g)	18.71	28.94	42.36	18.24	15.45
$k_1$ ( $\text{min}^{-1}$ )	0.032	0.047	0.033	0.035	0.033
$R^2$	0.9702	0.9591	0.9914	0.9727	0.9856
<b>Pseudo-second-order kinetic</b>					
$q_e$ (mg/g)	16.13	22.04	29.27	22.27	20.69
$k_2$ ( $\text{g mg}^{-1} \text{min}^{-1}$ )	0.027	0.027	0.036	0.034	0.031
$R^2$	0.9934	0.9915	0.9952	0.9870	0.9850
<b>Intraparticle diffusion</b>					
$k_{id}$ ( $\text{min}^{1/2}$ )	1.21	1.44	1.48	1.52	1.89
C	7.24	8.60	11.75	11.13	9.99
$R^2$	0.9558	0.9220	0.7580	0.8137	0.7351

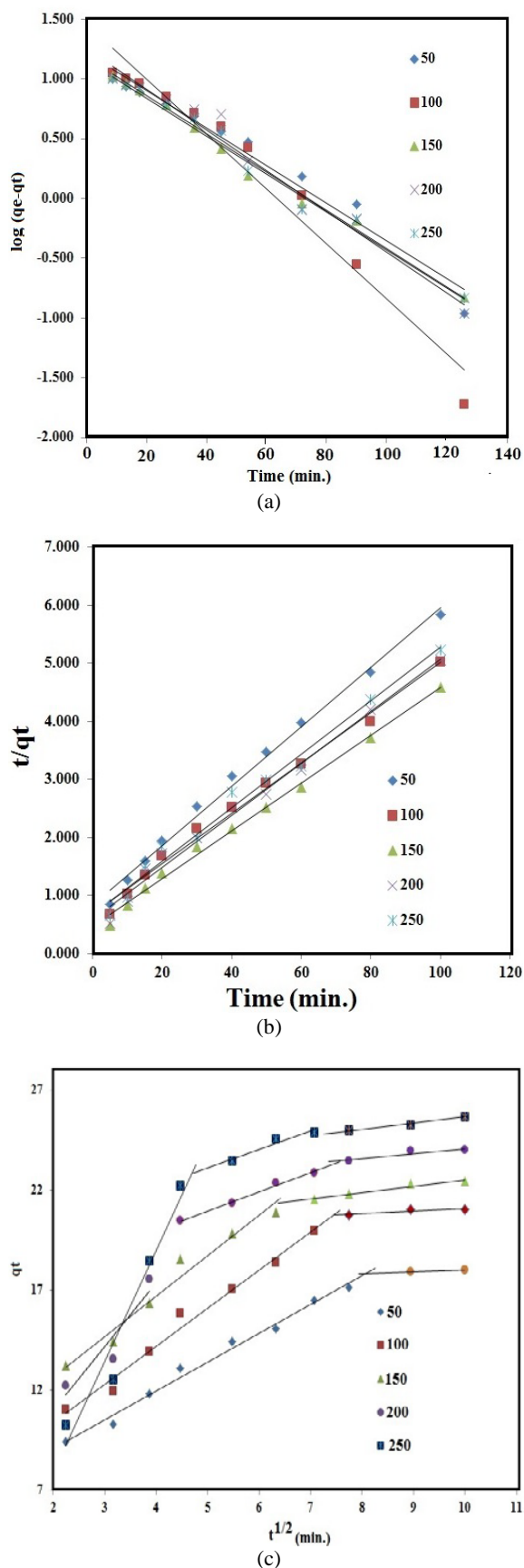


**Fig. 6.** Kinetic plots for MO adsorption onto OPTP at different initial MO concentrations; (a) Pseudo-first-order kinetic plot (b) Pseudo-second-order kinetic plot and (c) Intraparticle diffusion plot

The values of the kinetics parameter for pseudo second order were calculated from linear plots ( $t/q_t$ ) vs  $t$  (Fig. 6b). The obtained values for kinetic parameters are tabulated in Table 3. From the results, the values of correlation coefficient ( $R^2$ ) for pseudo-second-order are higher than for pseudo-first-order. These results demonstrate that adsorption of MO onto OPTP followed the pseudo-second-order kinetics. Similar results for the adsorption of MO have been reported by Hosseini et al. (2011) and Cheah et al. (2013).

To investigate the diffusion mechanism of MO onto OPTP, Weber-Morris intraparticle diffusion model was examined. The linear equation for intraparticle diffusion model is as follows (Eq. 4):

$$q_t = k_{id} t^{1/2} + C \quad (4)$$

where,  $q_t$  is the amount adsorbed ( $\text{mg g}^{-1}$ ) at time  $t$  (min),  $k_{id}$  is the diffusion rate constant ( $\text{mg g}^{-1}\text{min}^{1/2}$ ) and  $C$  is a constant ( $\text{mg g}^{-1}$ ).

The value of  $k_{id}$ ,  $C$  and  $R^2$  were calculated from the slope of plot  $q_t$  vs  $t^{1/2}$  as shown in Fig. 6c and data presented in Table 3. It shows the multi-linearity for MO adsorption onto OPTP, implying more than one rate determining steps were involved in adsorption process. First linear region is attributed to external diffusion (film diffusion) of MO onto the OPTP surface and second linear portion belongs to the intraparticle diffusion of MO, as a delayed process. Furthermore, plot shown in Fig. 6c reveals that there are few steps playing an important role in the adsorption process due to the multi-linearity correlation. There is deviation in line which does not pass through the origin, indicates that film diffusion and intraparticle diffusion were involved in the adsorption process (Cheung et al., 2007).

### 3.5. Adsorption isotherm

The surface property, affinity of adsorbent and adsorbate have been characterized by using three isotherm models viz., Langmuir (Langmuir, 1918), Freundlich (Freundlich, 1907) and Temkin (Temkin and Pyzhev, 1940) in order to determine the most suitable model which represents the adsorption process. The Langmuir model speculates that adsorption occurs at homogeneous sites on the adsorbents and monolayer coverage of the adsorbate at the outer surface of the adsorbents while the Freundlich model is employed to describe the nonideal adsorption on heterogenous surfaces and multilayer adsorption which is characterized by the heterogeneity factor  $1/n$ . The adsorption of MO dyes onto OPTP was investigated at the various concentrations ranging from 50-250  $\text{mgL}^{-1}$  with fixed amount of adsorbents at temperatures 30, 45 and 60 °C. The result reveals that equilibrium uptake increases with the increase in metal ion concentration. The increase in the adsorption capacity relates to the MO concentration may be due to the high driving forces for mass transfer. The linearized form of Langmuir, Freundlich

and Temkin isotherm are represented as follows (Eqs. 5-7):

$$\frac{C_e}{q_e} = \frac{1}{q_m b} + \frac{C_e}{q_m} \quad (5)$$

$$\ln q_e = \ln K_F + \frac{1}{n} \ln C_e \quad (6)$$

$$q_e = B \ln A + B \ln C \quad (7)$$

where,  $C_e$  is the equilibrium concentration ( $\text{mgL}^{-1}$ ),  $q_e$  is the amount biosorbed at equilibrium ( $\text{mgg}^{-1}$ ) and  $q_m$  and  $b$  is Langmuir constants related to biosorption efficiency and energy of biosorption, respectively.

A plot of  $C_e/q_e$  vs  $C_e$  should be a straight line with a slope  $1/q_m$  and an intercept  $1/bq_m$  as shown in Fig. 7a. The Freundlich constant  $K_F$  and  $1/n$  are related to the adsorption capacity and heterogeneity factors related to binding strength, respectively. As shown in Fig. 7b, a plot of  $\ln q_e$  vs  $\ln C_e$  should be a straight line with a slope  $1/n$  and an intercept of  $\ln K_F$ .  $A$  is equilibrium binding constant ( $\text{L mg}^{-1}$ ) and  $B$  is related to the heat of biosorption. A plot of  $q_e$  vs  $\ln C_e$  gives a linear line as shown in Fig. 7c. The values of isotherm parameters were calculated from the slope and intercept of their respected plots. The isotherm parameters are presented in Table 4.

**Table 4.** The related parameters for the adsorption of MO on OPTP at different temperatures

Adsorption Isotherms and its Constants	Temperatures ( $^{\circ}\text{C}$ )		
	30	45	60
<b>Langmuir Adsorption Isotherm Constants</b>			
$q_m$ (mg/g)	119.04	114.94	147.05
$b$ (L/mg)	0.044	1.450	0.250
$R^2$	0.9961	0.9887	0.9936
$R_L$	0.312	0.013	0.074
<b>Freundlich Adsorption Isotherm Constants</b>			
$K_F$ (mg/g) ( $\text{L/mg})^{1/n}$	19.80	16.63	16.95
$1/n$	0.6937	0.7418	0.7291
$R^2$	0.8954	0.9445	0.9281
<b>Temkin Adsorption Isotherm Constants</b>			
$A$ (L/mg)	45.56	37.21	48.27
$B$	6.927	7.355	7.1258
$R^2$	0.9774	0.9757	0.9836

The correlation coefficient ( $R^2$ ) of the Langmuir isotherm is relatively high [0.9961, 0.9887 and 0.9936] as compared to Freundlich [0.8954, 0.9445 and 0.9281] and Temkin [0.9774, 0.9757 and 0.9836] isotherm models at different temperature 30, 45 and 60  $^{\circ}\text{C}$ , respectively. From the results it can be concluded that regression coefficient ( $R^2$ ) values as obtained by linearized isotherms showed better fitting of experimental data to Langmuir isotherm. Therefore, it was confirmed that MO adsorption onto OPTP surface is homogeneously with constant energy and no transmission of MO in the plane of surface. In present work, used adsorbent OPTP has higher monolayer

capacity which is superior in comparison to other previous reported work (Table 5) such as De-Oiled Soya and Bottom ash (Mittal et al., 2007), Banana peel and Orange peel (Annadurai et al., 2002), Hypercrosslinked polymer (Huang et al., 2008) except Calcined layered double hydroxides (Ni et al., 2007).

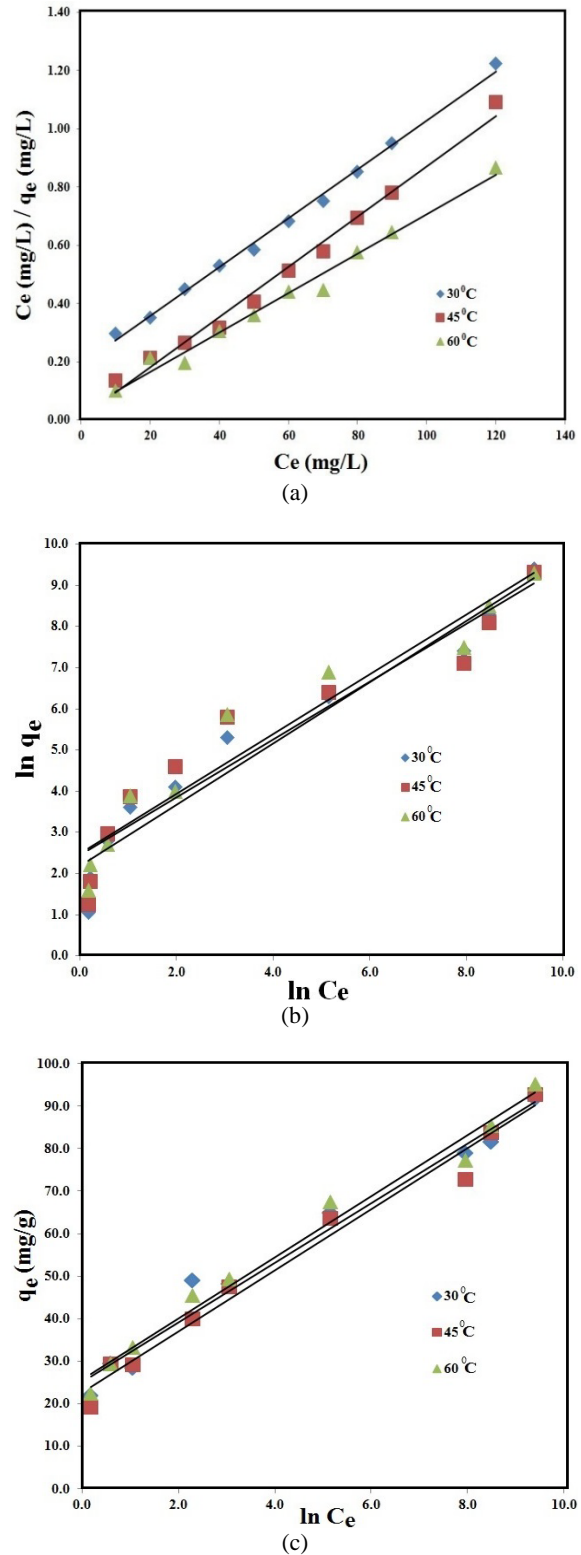


**Fig. 7.** Isotherm plots for MO adsorption onto OPTP at different temperatures; (a) Langmuir isotherm plot (b) Freundlich isotherm plot and (c) Temkin isotherm plot



**Table 5.** Comparison of adsorption capacities and other parameters of various adsorbents for MO

Adsorbents	Adsorption capacity	Contact time	Conc. range	pH	Temp. range	References
De-Oiled Soya	16.664 mg/g	150 min	$1 \times 10^{-5}$ - $10 \times 10^{-5}$ M	3	30-50 (°C)	Mittal et al. (2007)
Bottom ash	3.618 mg/g	4 h	$1 \times 10^{-5}$ - $10 \times 10^{-5}$ M	3	30-50 (°C)	Mittal et al. (2007)
Ammonium-functionalized MCM-41	1.12 mmol/g	240 min	0.21- 0.42 mmol/L	5.6	24.5±0.5 (°C)	Qin et al. (2009)
Banana peel	21 mg/g	65 min	10-120 mg/L	5.7	30 (°C)	Annadurai et al. (2002)
Orange peel	20.5 mg/g	65 min	10-120 mg/L	5.7	30 (°C)	Annadurai et al. (2002)
Calcined layered double hydroxides	181.9 mg/g	120 min	50-200 mg/L	6	25-65 (°C)	Ni et al. (2007)
Coconut shell fibers based AC	$2.88 \times 10^{-5}$ mol/g	24 hrs	$1 \times 10^{-5}$ - $1 \times 10^{-4}$ M	4	30-50 (°C)	Singh et al. (2003)
Hypercrosslinked polymer	20-50 mg/g	24 hrs	100-600 mg/L	NA	20-40 (°C)	Huang et al. (2008)
Oil palm trunk powder (OPTP)	119.04-147.05 mg/g	120 min	50-250 mg/L	6.0	30-60 (°C)	This study

The adsorption of MO was also characterized by Vermeulan criteria (Hall et al., 1966) associated with the Langmuir isotherm. The Vermeulan criteria are expressed by diamention less separation fraction " $R_L$ ", represented by the following equation (Eq. 8):

$$R_L = 1/(1 + bC_0) \quad (8)$$

where,  $C_0$  ( $\text{mgL}^{-1}$ ) is the initial metal ion concentration and  $b$  ( $\text{Lmg}^{-1}$ ) is Langmuir constant. The value of  $R_L$  indicates the shape of isotherms to be either:  $R_L > 1$  for unfavorable biosorption,  $R_L = 1$  for linear biosorption,  $0 < R_L < 1$  for favorable biosorption, and  $R_L = 0$  for irreversible adsorption. The values of  $R_L$  are in the range of 0.013 to 0.312 for MO indicating that the adsorption was favorable. Comparison of adsorption capacity and other parameters of OPTP and other adsorbents for the removal of MO from aqueous solution are tabulated in Table 5.

### 3.6. Determination of thermodynamic parameters

In order to assess the thermodynamic parameters for MO removal such as standard free energy change ( $\Delta G^\circ$ ), entropy change ( $\Delta S^\circ$ ) and enthalpy change ( $\Delta H^\circ$ ) were calculated using following equations (Eqs. 9 and 10):

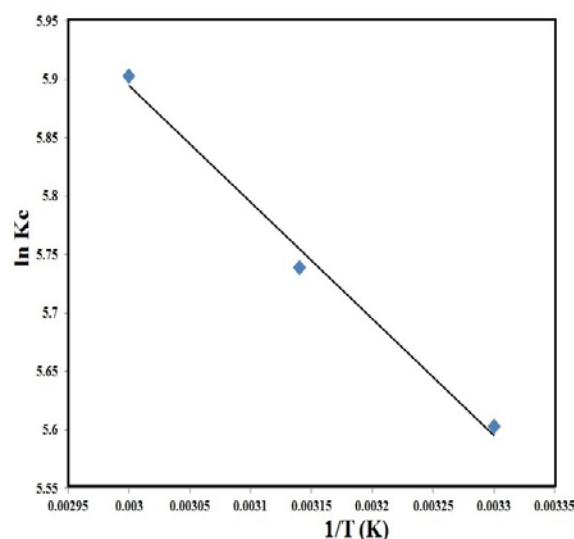
$$\Delta G^\circ = -RT \ln K_c \quad (9)$$

$$\ln K_c = \frac{\Delta S^\circ}{R} - \frac{\Delta H^\circ}{RT} \quad (10)$$

where,  $T$  (K) is the absolute temperature and  $R$  ( $8.314 \text{ J mol}^{-1} \text{ K}^{-1}$ ) is universal gas constant and  $K_c$  is the distribution coefficient.

The values of enthalpy change ( $\Delta H^\circ$ ) and entropy change ( $\Delta S^\circ$ ) were calculated from the slope and intercept of  $\ln K_c$  vs  $1/T$  plot for the adsorption of

MO onto OPTP at various temperature, which is presented in Fig. 8. From the Table 6, the value of  $\Delta G^\circ$  varies from -14.11 to -16.34  $\text{kJ mol}^{-1}$  with temperature rising from 303 to 333 K and the negative value of  $\Delta G^\circ$  indicates the feasibility and spontaneous nature of adsorption with high performance of MO for OPTP. The positive values of  $\Delta H^\circ$  indicates the adsorption process is endothermic in nature, while positive  $\Delta S^\circ$  values confirmed the increase disorderness at solid/solution interface during adsorption process of MO onto OPTP (Hosseini et al., 2011). The energy associated with different physical forces such as van der Waals forces (4-10  $\text{kJ/mol}$ ), hydrophobic bond forces (5  $\text{kJ/mol}$ ), hydrogen bond forces (2-40  $\text{kJ/mol}$ ), coordination exchange (40  $\text{kJ/mol}$ ), dipole bond forces (2-29  $\text{kJ/mol}$ ) and for chemical forces ( $>60 \text{ kJ/mol}$ ) (Mattson and Mark, 1971). In this study,  $\Delta H^\circ$  was found 19.07  $\text{kJ/mol}$ , revealed that physical forces were involved in adsorption of MO onto OPTP.

**Fig. 8.** Plot of  $\ln K_c$  vs  $1/T$  for MO adsorption onto OPTP

**Table 6.** Values of thermodynamic parameters for MO adsorption onto OPTP

Temp. (K)	$\Delta G^\circ$ (kJmol <sup>-1</sup> )	$\Delta H^\circ$ (kJmol <sup>-1</sup> )	$\Delta S^\circ$ (kJmol <sup>-1</sup> K <sup>-1</sup> )	R <sup>2</sup>
303	-14.11	19.07	73.85	0.9915
318	-15.17			
333	-16.34			

#### 4. Conclusions

The intent of this study was to find the proper adsorption mechanism of MO dyes onto acid treated OPTP material. The adsorption of MO onto OPTP was strongly pH dependent. In acidic medium adsorption occurs by electrostatic, hydrogen bonding and hydrophobic-hydrophobic interactions. Carboxylic (COO<sup>-</sup>) and hydroxyl (OH) functional groups present on OPTP plays an important role for the MO adsorption. Thermodynamic studies showed that adsorption of MO onto OPTP were spontaneous and endothermic in nature. The OPTP material will be promising, alternative, economical and effective adsorbents for the removal of MO dyes from wastewater.

#### Acknowledgements

The authors acknowledge the research grant provided by the Universiti Sains Malaysia under the Short Term Grant Scheme (Project No. 304/PTEKIND/6312118).

#### References

- Abou-El-Souod G.W., El-Sheekh M.M., (2016), Biodegradation of basic fuchsin and methyl red by the blue green algae hydrocoleum oligotrichum and oscillatoria limnetica, *Environmental Engineering and Management Journal*, **15**, 279-286.
- Ahmad A., Rafatullah M., Sulaiman O., Ibrahim M.H., Hashim R., (2009), Scavenging behaviour of meranti sawdust in the removal of methylene blue from aqueous solution, *Journal of Hazardous Materials*, **170**, 357-365.
- Ahmad R., (2009), Studies on adsorption of crystal violet dye from aqueous solution onto coniferous pinus bark powder (CPBP), *Journal of Hazardous Materials*, **171**, 767-773.
- Ahmad R., Kumar R., (2010), Adsorptive removal of congo red dye from aqueous solution using bael shell carbon, *Applied Surface Science*, **257**, 1628-1633.
- Ahmad T., Rafatullah M., Ghazali A., Sulaiman O., Hashim R., (2011), Oil Palm Biomass-Based Adsorbents for the Removal of Water Pollutants-A Review, *Journal of Environmental Science and Health, Part C*, **29**, 177-222.
- Allen S.J., McKay G., Porter J.F., (2004), Adsorption isotherm models for basic dye adsorption by peat in single and binary component system, *Journal of Colloid and Interface Science*, **280**, 322-333.
- Annadurai G., Juang R.S., Lee D.J., (2002), Use of cellulose-based wastes for adsorption of dyes from aqueous solutions, *Journal of Hazardous Materials*, **B92**, 263-274.
- Ashtouky E.S.Z.E., (2009), Loofa egyptiaca as a novel adsorbent for removal of direct blue dye from aqueous solution, *Journal of Environmental Management*, **90**,

2755-2761.

- Atmani F., Bensmaili A., Mezenner N.Y., (2009), Synthetic textile effluent removal by skin almonds waste, *Journal of Environmental Science Technology*, **2**, 153-169.
- Ayar A., Gezici O., Kucukosmanoglu M., (2007), Adsorptive removal of Methylene blue and Methyl orange from aqueous media by carboxylated diaminoethane sporopollenin: On the usability of an aminocarboxylic acid functionality-bearing solid-stationary phase in column techniques, *Journal of Hazardous Materials*, **146**, 186-193.
- Cheah W., Hosseini S., Khan M. A., Chuah T.G., Choong T.S.Y., (2013), Acid modified carbon coated monolith for methyl orange adsorption, *Chemical Engineering Journal*, **215-216**, 747-754.
- Cheung W.H., Szeto Y.S., McKay G., (2007), Intraparticle diffusion processes during acid dye adsorption onto chitosan, *Bioresource Technology*, **98**, 2897-2904.
- Cretescu I., Diaconu M., Dughila A., Stefanache A., Pohontu C., (2010), Studies on the biosorption of Terasil dye by Aspergillus niger dead biomass, *Environmental Engineering and Management Journal*, **9**, 335-340.
- Demarchi C.A., Debrassi A., Rodrigues C.A., (2016), Use of chitosan-iron(iii) for the adsorption of the dye acid red 29: isotherm, kinetic, reuse and factorial design, *Environmental Engineering and Management Journal*, **15**, 2441-2451.
- Freundlich H., (1907), Adsorption in solution (in Germany), *Journal of Physical Chemistry*, **57**, 385-470.
- Gong R., Zhong K., Hu Y., Chen J., Zhu G., (2008), Thermochemical esterifying citric acid onto lignocellulose for enhancing methylene blue sorption capacity of rice straw, *Journal of Environmental Management*, **88**, 875-880.
- Gupta V.K., Ali I., Saleh T.A., Nayak A., Agarwal S., (2012a), Chemical treatment technologies for wastewater recycling - an overview, *RSC Advances*, **2**, 6380-6388.
- Gupta V.K., Jain R., Mittal A., Saleh T.A., Nayak A., Agarwal S., Sikarwar S., (2012b), Photo-catalytic degradation of toxic dye amaranth on TiO<sub>2</sub>/UV in aqueous suspensions, *Materials Science and Engineering C*, **32**, 12-17.
- Hall K.R., Eagleton L.C., Acrivos A., Vermeulen T., (1966), Pore and solid diffusion kinetics in fixed bed adsorption under constant pattern conditions, *Industrial and Engineering Chemistry Fundamentals*, **5**, 212-219.
- Hameed B.H., Mahmoud D.K., Ahmad A.L., (2008), Sorption of basic dye from aqueous solution by pamele (Citrus grandis) peel in batch system, *Colloids and Surfaces A: Physicochemical and Engineering Aspects*, **316**, 78-84.
- Hosseini S., Khan M.A., Malekbala M.R., Cheah W., Choong T.S.Y., (2011), Carbon coated monolith, a mesoporous material for the removal of methyl orange from aqueous phase: Adsorption and desorption studies, *Chemical Engineering Journal*, **171**, 1124-1131.
- Huang J.H., Huang K.L., Liu S.Q., Wang A.T., Yan C., (2008), Adsorption of Rhodamine B and methyl orange on a hypercrosslinked polymeric adsorbent in aqueous solution, *Colloids and Surfaces A: Physicochemical and Engineering Aspects*, **330**, 55-61.
- Janos P., Agapovova E., Fikarova J., Sedlbauer J., Janos Jr P., (2016), Biosorption of sulfonic azodyes on spruce wood shavings: kinetics and sorption mechanisms, *Environmental Engineering and Management Journal*, **15**, 2671-2680.

- Kannan C., Buvanewari N., Palvannan T., (2009), Removal of plant poisoning dyes by adsorption on tomato plant root and green carbon from aqueous solution and its recovery, *Desalination*, **249**, 1132-1138.
- Kumar R., Barakat M.A., (2013), Decolorization of hazardous brilliant green from aqueous solution using binary oxidized cactus fruit peel, *Chemical Engineering Journal*, **226**, 377-383.
- Lagergren S., (1898), About the theory of so-called adsorption of soluble substances (in Germany), *Kungliga Svenska Vetenskapsakademiens Handlingar*, **24**, 1-39.
- Langmuir I., (1918), The sorption of gases on plane surfaces of glass, mica and platinum, *Journal of American Chemical Society*, **40**, 1361-1403.
- Lucaci D., Duta A., (2011), Removal of methyl orange and methylene blue dyes from wastewater using sawdust and sawdust-fly ash as sorbents, *Environmental Engineering and Management Journal*, **10**, 1255-1262.
- Lutic D., Coromelci C.-G., Juzsakova T., Cretescu I., (2017), New mesoporous titanium oxide-based photoactive materials for the removal of dyes from wastewaters, *Environmental Engineering and Management Journal*, **16**, 801-807.
- Machado F.M., Bergmann C.P., Lima E.C., Royer B., de Souza F.E., Jauris I.M., Calvete T., Fagan S.B., (2012), Adsorption of reactive blue 4 dye from water solutions by carbon nanotubes: Experiment and theory, *Chemistry Chemical Physics*, **14**, 11139-11153.
- Malik P.K., Sanyal S.K., (2004), Kinetics of decolourisation of azo dyes in wastewater by UV/H<sub>2</sub>O<sub>2</sub> process, *Separation and Purification Technology*, **36**, 167-175.
- Mattson J., Mark H., (1971), *Activated Carbon: Surface Chemistry and Adsorption from Carbon*, Marcel Dekker, Ins., New York.
- McKay G., Ho Y.S., (1999), Pseudo-second order model for sorption processes, *Process Biochemistry*, **34**, 451-465.
- Mittal A., Kaur D., Malviya A., Mittal J., Gupta V.K., (2009a), Adsorption studies on the removal of coloring agent phenol red from wastewater using waste materials as adsorbents, *Journal of Colloid and Interface Science*, **337**, 345-354.
- Mittal A., Krishnan L., Gupta V.K., (2005), Removal and recovery of malachite green from wastewater using an agricultural waste material, de-oiled soya, *Separation and Purification Technology*, **43**, 125-133.
- Mittal A., Malviya A., Kaur D., Mittal J., Kurup L., (2007), Studies on the adsorption kinetics and isotherms for the removal and recovery of Methyl Orange from wastewaters using waste materials, *Journal of Hazardous Materials*, **148**, 229-240.
- Mittal A., Mittal J., Malviya A., Gupta V.K., (2009b), Adsorptive removal of hazardous anionic dye "Congo red" from wastewater using waste materials and recovery by desorption, *Journal of Colloid and Interface Science*, **340**, 16-26.
- Mittal A., Mittal J., Malviya A., Gupta V.K., (2010b), Removal and recovery of Chrysoidine Y from aqueous solutions by waste materials, *Journal of Colloid and Interface Science*, **344**, 497-507.
- Mittal A., Mittal J., Malviya A., Kaur D., Gupta V.K., (2010a), Decoloration treatment of a hazardous triarylmethane dye, Light Green SF (Yellowish) by waste material adsorbents, *Journal of Colloid and Interface Science*, **342**, 518-527.
- Mondal P.K., Ahmad R., Kumar R., (2014), Adsorptive removal of hazardous methylene blue by fruit shell of *Cocos nucifera*, *Environmental Engineering and Management Journal*, **13**, 231-240.
- Ni Z.M., Xia S.J., Wang L.G., Xing F.F., Pan G.X., (2007), Treatment of methyl orange by calcined layered double hydroxides in aqueous solution: Adsorption property and kinetic studies, *Journal of Colloid and Interface Science*, **316**, 284-291.
- Qin Q., Ma J., Liu K., (2009), Adsorption of anionic dyes on ammonium-functionalized MCM-41, *Journal of Hazardous Materials*, **162**, 133-139.
- Saleh T.A., Gupta V.K., (2012), Photo-catalyzed degradation of hazardous dye methyl orange by use of a composite catalyst consisting of multi-walled carbon nanotubes and titanium dioxide, *Journal of Colloid and Interface Science*, **371**, 101-106.
- Singh K.P., Mohan D., Sinha S., Tondon G.S., Gosh D., (2003), Color removal from wastewater using low-cost activated carbon derived from agricultural waste material, *Industrial and Engineering Chemistry Research*, **42**, 1965-1976.
- Sjöström E., (1981), *Wood Chemistry: Fundamentals and Applications*, Gulf Professional Publishing, San Diego, USA.
- Suteu D., Rusu L., (2012), Removal of methylene blue dye from aqueous solution using seashell wastes as biosorbent, *Environmental Engineering and Management Journal*, **11**, 1977-1986.
- Tan I.A.W., Hameed B.H., Ahmad A.L., (2007), Equilibrium and kinetic studies on basic dye adsorption by oil palm fibre activated carbon, *Chemical Engineering Journal*, **127**, 111-119.
- Temkin M.I., Pyzhev V., (1940), Kinetics of ammonia synthesis on promoted iron catalysts, *Acta Physicochemica SSR*, **12**, 217-222.
- Wang L., Wang A., (2008), Adsorption properties of congo red from aqueous solution onto surfactant-modified montmorillonite, *Journal of Hazardous Materials*, **160**, 173-180.
- Weber Jr.W.J., Morris J.C., (1963), Kinetics of adsorption on carbon from solution, *Journal of the Sanitary Engineering Division ASCE*, **89**, 31-59.
- Zhuannian L., Anning Z., Guirong W., Xiaoguang Z., (2009), Adsorption behavior of methyl orange onto modified ultrafine coal powder, *Chinese Journal of Chemical Engineering*, **17**, 942-948.